

AUTOMATED NEAR-REAL TIME IDENTIFICATION AND CALCULATION OF AREA-BASED EMISSIONS

Chaim Kolominskas, Peter D'Abreton and Danny Craggs

Envirosuite, Brisbane, 4000, Australia

Abstract

Near-field, near real-time and predictive air quality modelling and management systems were first adopted by mining, minerals processing, wastewater treatment and governmental organisations 10 to 15 years ago to drive improvements in air quality management. In that time, the amount of continuous monitoring data available has also increased, allowing for the possibility of more automated identification and calculation of emissions from facilities. Automated calculation of emissions, if sufficiently accurate, can deliver both rapid identification of the location of current or emerging air quality issues, as well as improved accuracy of emission rates used in real-time or predictive modelling.

This paper describes an approach to source characterisation and emission estimation that uses continuous ambient air quality data and spatial data to back-calculate flux of emissions from a gridded field. The method used recalculates concentration data as gridded data to represent a concentration on all four sides (or faces) of each defined source or sub-source. Emissions for the sources are then calculated using a modified version of the model, where x- and y-components of the wind are separately used for emission estimation.

Two examples are presented in this paper 1) The “Gridding method” where emissions are highly variable in time and space over a large area where there is an extensive monitoring network (mine). 2) A “Simple method” applied for smaller, simpler sources where the monitoring network is inadequate to produce an accurate gridded field (port).

Keywords: Automated emissions calculation

1. Introduction

Near-field, near real-time and predictive air quality modelling and management systems were first adopted by mining, minerals processing, wastewater treatment and governmental organisations 10 to 15 years ago to drive improvements in air quality management.

Initially, monitoring, if present at all, was limited to one or a few regulatory standard (i.e. higher accuracy) monitors at each site. The focus of monitoring was traditionally regulatory reporting, with reports prepared at periodic intervals for inclusion in corporate reporting or submission to local regulators.

Over time, a greater number of lower-cost air quality monitoring devices became available, with improved reliability and accuracy and improved understanding of how best to manage the limitations of those types of devices (Carotenuto et. al., 2023). At the same time, the costs of cloud-based computing and storage decreased, and most air quality monitoring networks are these days available for near real-time access.

It is now much more common to see individual sites with relatively dense monitoring networks, or the willingness to invest in these networks to support an improvement in on-site air quality management. Similarly, regulatory authorities globally are investigating how best to complement the devices that they do have with denser networks of low-cost devices (e.g., Shatas & Hubbell, 2022).

Given the availability of air quality data, new possibilities for improved air quality management have emerged. To this end, the paper describes the theory of how data from multiple ambient monitoring devices can be used to identify and calculate emissions sources across an industrial site and then discusses the results of a subset of validation studies used in designing a commercial air quality management solution based on that science. Finally, the paper describes some of the key aspects design required to successfully apply the solution in practice.

2. Objective

The objective of applying the methods described in this paper were to:

- Rapidly and easily identify the location and magnitude of area based, non-buoyant emission sources across an industrial facility. It was important to be able to identify both known and unknown sources.
- Estimate emissions at a resolution useful for near real-time input into a dispersion model that significantly improves calculation of off-site impacts.

3. Methodology

The approach used comprises the sequential application of two key elements, gridding and emissions modelling, which are both described in this section.

3.1. Gridding

The monitoring data at most industrial operations is scattered across the facility area in an irregular distribution. This results in some areas having excellent monitor coverage whereas other areas do not have adequate coverage. The initial step of the calculation process therefore involves resolving monitored emissions into a regular, gridded distribution using the Kriging approach.

Kriging is the most used geostatistical approach for gridding data and relies on a spatial model between observations to predict attribute values at unsampled locations. More specifically, Kriging fits a mathematical function to points within a specified radius to determine the output value for each location. The general formula for Kriging is given as a weighted sum of the data:

$$\hat{Z}_{(s_0)} = \sum_{i=1}^N \lambda_i Z_{si} \quad (1)$$

Where:

- $\hat{Z}_{(s_0)}$ = The total emissions from the area
- N = The number of measured values
- λ_i = A weighting factor based on the distance between the measured points and the prediction location and the overall spatial arrangement of the measured points
- $\hat{Z}_{(s_i)}$ = The measured value at location i

3.2. Emissions modelling

The gridded distribution then forms the basis of emissions modelling from each individual area source. The area is converted to a grid and emissions are calculated using a flux model approach.

Surface flux models are based on the conservation of mass and consists of multiple cubes placed over the source's surface to capture the emissions (Arya, 1999; Flocchini, et al., 2001). The emissions are subsequently transported through the downwind end of the box. Concentration measurements are made on the upwind and downwind ends of the box, with the net concentrations assumed to represent the contribution made by sources within each cube. A small-scale modification of the model was implemented where mass balances were performed using both u and v wind components. The equation below shows how the flux is calculated using this model.

$$Q_A = \left[\frac{U \times y \times h \times C}{x \times y} \right] + \left[\frac{V \times y \times h \times C}{x \times y} \right] \quad (2)$$

Where:

Q_A	=	Emission flux	$\mu\text{g}/\text{m}^2.\text{s}$
U	=	Measured u-component of wind	m/s
V	=	Measured v-component of wind	m/s
h	=	Plume height	m
C	=	Net measured concentration (less background)	$\mu\text{g}/\text{m}^3$
x	=	Upwind length of the box	m

Given concentration data across a network of sensors and representative wind speed and wind direction data across the monitoring area, it is therefore possible to calculate the flux of emissions from each predefined grid square across the area.

3.3. Case studies

Two case studies where this approach has been applied and assessed are shared in this paper – a mine (18 monitors) and a port (10 monitors). In both cases, hourly calculated emission rates and ambient concentrations are compared with measured concentrations.

4. Results

Calculated emission rates ($\text{g}/\text{m}^2/\text{s}$) were investigated for a large mining area and a more compact port.

4.1. Mine

The monitoring data over the mine was gridded, transforming the mine into equal areas (Figure 1). The emission rates for each area were calculated according to Equation 1. Figure 2 shows calculated area emissions flux for a snapshot in time. Activity-based emissions are clearly evident in the figure.

The accuracy of the calculated emissions was tested by comparing modelled and measured 24-hour

average and 1-hour maximum PM₁₀ concentration at the ambient monitors (Figure 3). The model predicts both 24-hour average and 1-hour maxima well at monitors 1, 2, and 4. The model underprediction at the more distant Monitor 3. This is most likely due to other unaccounted for sources in the area.

Correlation fields between calculated area emission fluxes and Monitor 1 is presented in Figure 4. Significant positive correlations occur between emission rates over the western parts of the mine and ambient concentrations at the monitor.

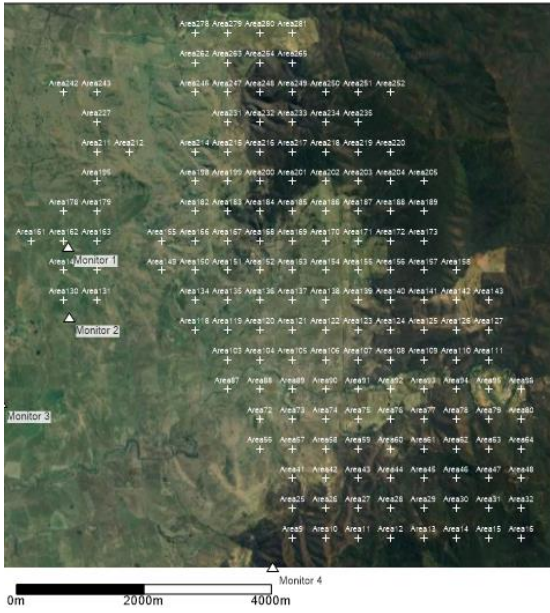


Figure 1: Gridded source areas

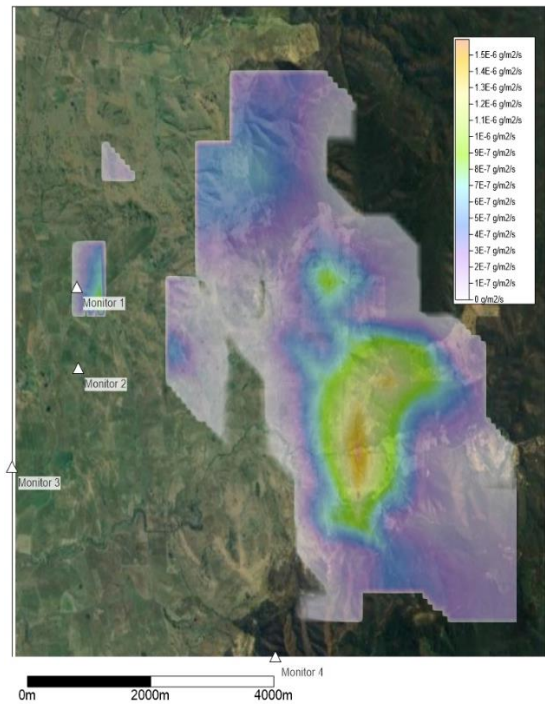


Figure 2: Calculated emissions rates at a mine

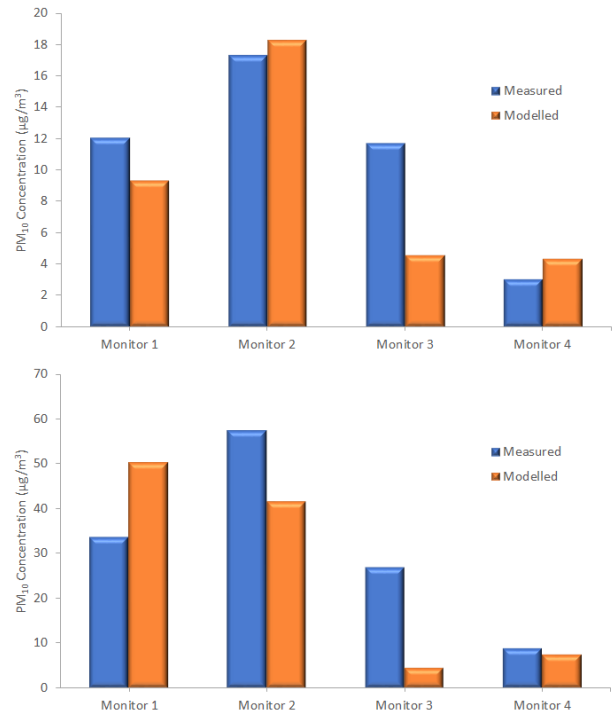


Figure 3: Modelled versus measured 24-hour average (top) and maximum 1-hour concentration (bottom).

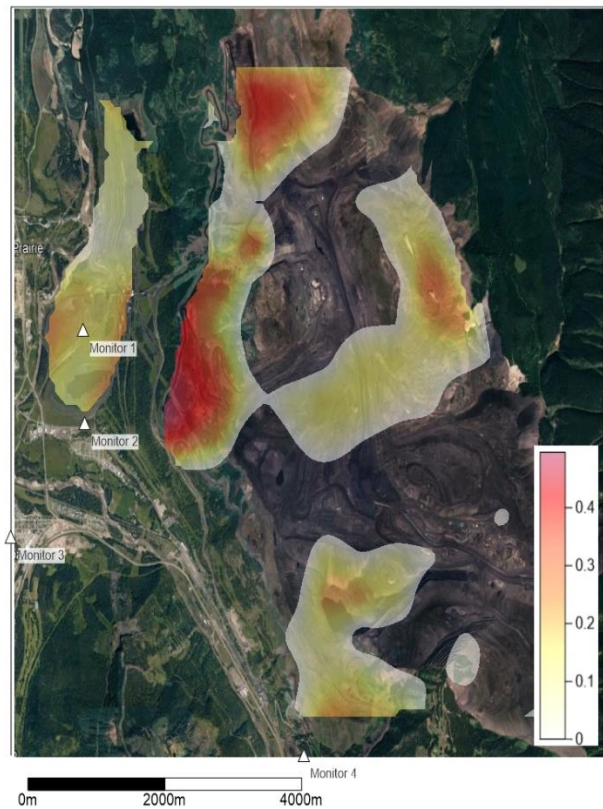


Figure 4: Correlation fields of calculated emissions and PM₁₀ concentration at Monitor 1

The ordinary least squares (OLS) method is a statistical procedure to find the best fit for a set of data points by minimising the sum of the offsets or residuals of points from the plotted curve and provides the overall rationale for the placement of the line of best fit among the data points being studied. The coefficient for each explanatory variable reflects both the strength and type of relationship the explanatory variable has to the dependent variable. When the sign associated with the coefficient is negative, the relationship is negative, and when the sign is positive, the relationship is positive. For a 95 percent confidence level, a p-value (probability) smaller than 0.05 indicates a statistically significant model.

Table 1 shows the coefficients (significant at the 95 per cent level) between various meteorological variable and emission source areas (Figure 1):

- Pressure, wind speed, u- and v-components of wind, relative humidity and certain emission areas have significant coefficients at Monitor 1. The results suggest increased ambient PM₁₀ concentrations occurring with increased pressure and increased v-component of wind, decreased wind speed, u-component (easterly), and relative humidity. Higher PM₁₀ concentrations are related to increased emissions in areas to the north of the site. A correlation coefficient of 0.86 indicates a good performance of the data in the OLS model.
- At the Monitor 2, significant coefficients occur with emissions from two main areas of the mine. A correlation coefficient of 0.78 indicates a good performance of the data in the OLS model.
- Relative humidity and temperature areas have significant positive OLS coefficients at Monitor 4, indicating increased PM₁₀ concentration with increased relative humidity and temperature. Conversely, pressure, wind speed and v- (north-south) component of wind have significant negative OLS coefficients. This suggests increased ambient PM₁₀ measurement at the monitor with lower atmospheric pressure and increased northerly wind component. A correlation coefficient of 0.98 indicates excellent performance of the data in the OLS model.

4.2. Port

The calculated near-surface emission fluxes from a fictional port were determined from a network of monitors shown in Figure 5. Three potential sources of PM₁₀ emissions were proposed to allow for potential targeted mitigation responses.

Figure 6 shows the calculated emission rates from the three areas, with Area A producing significantly higher emissions, followed by Area C. This is most likely reflecting activity-based emissions occurring over certain parts of the port.

Table 1: Significant coefficients from the OLS model

Monitor 1		Monitor 2		Monitor 4	
Press.	0.6	Area44	2.0	RH	1.1
Wspd	-0.4	Area56	0.6	Press.	-0.5
U-comp	-0.2	Area134	0.8	Temp	4.7
V-comp	0.3	Area182	0.9	Wspd	-1.9
RH	-0.4	Area183	1.0	V-comp	-0.9
Area165	1.6			Area44	2.6
Area263	3.7			Area75	0.5
				Area76	0.6
				Area110	0.3
				Area30	2.2
				Area172	3.0
				Area188	8.6
				Area149	13.8
				Area214	24.5
				Area147	10.2
corr	0.86	corr	0.78	corr	0.98



Figure 5: Ambient monitors and potential sources at a port.



Figure 6: Calculated emissions rates at a port

Correlation fields between calculated emissions from Area A and gridded ambient PM₁₀ concentration is shown in Figure 7. Highest correlation coefficients of 0.4 are found immediately to the west and northwest of the port area, with areas of significant positive correlations extending along the entire eastern length of the port. There is a lack of correlation between emissions and PM₁₀ concentration to the south, reflecting the prevailing winds in the area.

Correlation fields between Area B and gridded ambient monitors shows highest correlation of 0.5 occurring immediately to the east of the source area (Figure 8).

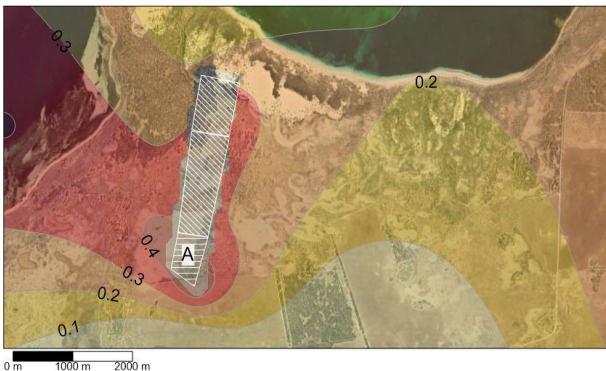


Figure 7: Correlation fields of calculated emissions (Area A) and ambient monitor concentrations

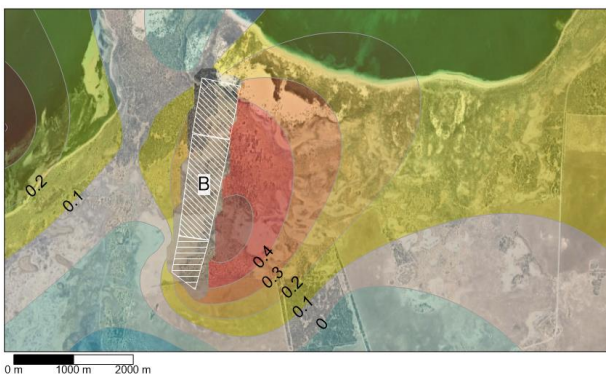


Figure 8: Correlation fields of calculated emissions (Area B) and ambient monitor concentrations

Correlation fields between calculated emissions from Area C (hatched) and gridded ambient PM₁₀ concentration is shown in Figure 9. As expected, highest positive correlations are found immediately adjacent to Area C although significant correlations (>0.2) occur across the northern part of the domain. There is again a lack of correlation between emissions and PM₁₀ concentration to the south.

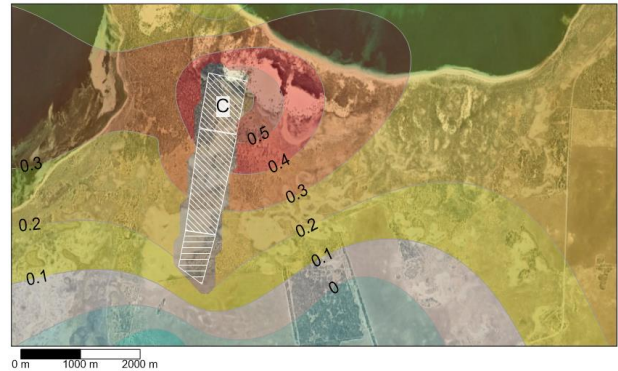


Figure 9: Correlation fields of calculated emissions (Area C) and ambient monitor concentrations

Table 2 show the OLS coefficients (significant at the 95 per cent level) at selected ambient monitors and emission source areas.

- Monitor 1 has higher ambient PM₁₀ concentrations associated with westerly and northerly wind components, and emissions from Area B (central part of the port). A correlation coefficient of 0.77 indicates relatively good performance of the data in the OLS model.
- Monitor 2 has higher ambient PM₁₀ concentrations associated with easterly and southerly component winds, and emissions from Area A (southern part of port). A correlation coefficient of 0.86 indicates good performance of the data in the OLS model.
- Monitor 3 has higher ambient PM₁₀ concentrations associated with strong, and easterly component winds, and emissions from Area B (central part of port). A correlation coefficient of 0.78 indicates relatively good performance of the data in the OLS model.
- Monitor 4 has higher ambient PM₁₀ concentrations associated with strong winds, and emissions from Area A (southern part of port). A correlation coefficient of 0.81 indicates relatively good performance of the data in the OLS model. A

Table 2: Significant coefficients from the OLS model – port

	Monitor 1	Monitor 2	Monitor 3	Monitor 4
Area A	-	0.01	-	0.02
Area B	0.02	-	0.03	-

Area C	-	-	-	-
Wind speed	-	5.94	13.11	7.21
u	8.63	-5.85	-13.12	-
v	-1.27	3.21	-	-
Correlation	0.77	0.86	0.78	0.81

5. Discussion

The results of this initial work are important in the field of real-time and predictive air quality management for several reasons. The initial results provided confidence that a much-improved representation of emissions from area-based, non-buoyant sources could be achieved, compared with traditional emission factor / activity-based approaches.

Once automated, visualised and integrated with alerting and response capabilities, the calculations of emissions in near real-time provides improved insights into current operations – namely the likely source of elevated impacts. If there is improved confidence in level of emissions across the site, it can be much easier to deploy control to the correct area and have the largest possible effect in reducing offsite impacts. A more accurate representation of emission rate can also significantly improve the accuracy of modelled impacts and leads to greater confidence in modelled based solutions.

These early results provided confidence that using a flux model and gridded approach would be a useful basis for new visualisation tools for air quality management at mines, ports and other industrial facilities where sufficient numbers of monitors are available.

The number of monitors needed depends on the type and scale of the site, as well as the intended use of the data. In some cases, it may be sufficient to use a few monitors and represent emissions from the site as a whole, or only some key emission sources. In other cases, are much higher resolution of monitors is needed to be able to differentiate between the different sources at a facility. It is also important to note that this approach only applies to non-buoyant sources. A site with a mixture of stack and area sources would need another method of understanding emissions from the site as a whole.

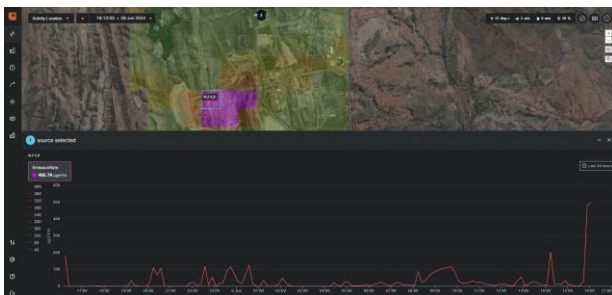


Figure 10: Automated area-based emission visualised for real-time and predictive management applications

6. Conclusions

This paper described an approach to source characterisation and emission estimation that uses continuous ambient air quality data, meteorological data and spatial data to back-calculate flux of emissions from a gridded field. The results of modelled impacts using emissions calculated in this new approach showed good correlation with measured data at both a mine and port.

Ultimately, this work led to further validation and calibration work with a number of sites around the world and the development of new real-time air quality management functionality within Envirosuite’s product suite. The underlying methodology and visualisation of data will be improved as initial customer engagements progress and the number of projects are expanded.

7. References

- Arya, S.P. (1999). *Air Pollution Meteorology and Dispersion*. Oxford University Press. New York.
- Carotenuto, F., Bisignano, A., Brilli, L., Gualtieri, G., & Giovannini, L. (2023). *Low-cost air quality monitoring networks for long-term field campaigns: A review*. *Meteorological Applications*, 30(6), e2161: <https://doi.org/10.1002/met.2161>
- Flocchini, R.G., T.A. James, L.L. Ashbaugh, M.S. Brown, O.F. Carvacho, B.A. Holmén, R.T. Matsumura, K. TrzeplaNabaglo, C. Tsubamoto. 2001. *Sources and Sinks of PM10 in the San Joaquin Valley – Interim Report*. United States Department of Agriculture Special Research Grants Program; Contract Nos. 94-33825-0383 and 98-38825-6063. Air Quality Group, Crocker Nuclear Laboratory, University of California, Davis.
- Shatas, A., Hubbell, B. (2022) *Using Low-Cost Sensor Networks: Considerations to Help Reveal Neighborhood-Level Exposure Disparities*, *American Journal of Public Health* 112, 1693_1695: <https://doi.org/10.2105/AJPH.2022.307128>